Effects of Approximating Recorded Lightning Currents With CIGRE Waveforms on Computed Fast-Front Overvoltages and Critical Lightning Currents Causing Flashover to Overhead Transmission Lines

Zacharias G. Datsios ⓘ, *Member, IEEE*, Diamantis G. Patsalis, *Graduate Student Member, IEEE*, Pantelis N. Mikropoulos ⓘ, *Senior Member, IEEE*, and Thomas E. Tsovilis ⓘ, *Senior Member, IEEE*

Abstract—This work investigates through simulations with the ATP-EMTP program the application of recorded lightning current waveforms to the estimation of fast-front overvoltages and critical lightning currents causing flashover to overhead transmission lines. Typical lines are evaluated with both horizontal (single-circuit) and vertical (double-circuit) phase configurations and AC voltage from 66 kV up to 765 kV. Backflashover as well as shielding failure flashover simulations were performed for several recorded first return-stroke current waveforms of negative downward lightning flashes, as reported in literature. Their approximations with the widely-used CIGRE lightning current waveform were also employed in simulations. CIGRE waveforms, considering the statistical distributions of the front time, maximum steepness, and time to half value, were used as well. A comparison between double-peak waveforms, composed of seven Heidler functions, and their CIGRE approximations is made. The latter generally yield conservative values of overvoltages and critical backflashover currents. The leader development models used for assessing the behavior of insulators and long air gaps under fast-front overvoltages are discussed regarding the criterion for the termination of leader propagation yielding withstand of line insulation.

Index Terms—Backflashover, EMTP, flashover, insulation coordination, leader progression models, lightning, shielding failure, overhead transmission lines.

I. INTRODUCTION

THE representation of the return-stroke phase of direct lightning strikes to overhead transmission lines (OHLs) affects considerably the simulated fast-front overvoltages stressing OHL insulation. Hence, it also affects the computed critical (minimum) lightning currents causing flashover of OHL

insulation and the estimated lightning performance of OHLs. This is in addition to other adopted modeling approaches and influencing parameters, including the geometry and dimensions of the grounding systems of towers and their representation, the electrical properties of soil, OHL and tower characteristics, and the employed flashover prediction method [1], [2], [3]. Thus, the estimation of lightning overvoltages, critical currents and of the lightning performance of OHL are demanding tasks investigated in several recent publications [4], [5], [6], [7], [8], [9], [10], [11], [12], [13], [14], [15], [16], [17], [18], [19], [20], [21], [22] due to the complexity involved.

When evaluating the effects of direct lightning strikes to objects on the ground, the lightning return-stroke is commonly represented by a Norton equivalent circuit, that is, a source generating the lightning current connected in parallel to the impedance representing the lightning channel [23], [24], [25], [26]. According to [12], this equivalent impedance is reported in literature to vary from $100\,\Omega$ to $10\,k\Omega$ (400-2500 Ω, based solely on field data obtained from instrumented towers) and affects considerably the estimated lightning flashover rate of OHLs, with higher impedances yielding conservative results. Thus, an ideal current source (infinite impedance) is often adopted [2], [26], [27], [28], [29]. Other values have been proposed as well, e.g., 400 Ω for backflashover and 1000 Ω for shielding failure investigations [12].

Regarding the lightning current, both simple and complex waveforms have been proposed and employed in investigations involving direct lightning strikes [28], [29], [30], [31], [32], [33], [34], [35], [36], [37], [38], [39] in order to approximate the characteristics of actual recorded lightning current waveforms and/or their most important effects on the system under study. Among the most common lightning current waveforms are the: i) triangular [30], [31], [32], ii) Heidler [33], [34], iii) CIGRE [28], [29], and iv) double-peak [29], [35] waveforms. The last two may replicate the upwardly concave wavefront of recorded first return-stroke currents of negative downward lightning flashes. The double-peak waveform may also reproduce the second higher peak usually observed at recorded currents. Hence, the
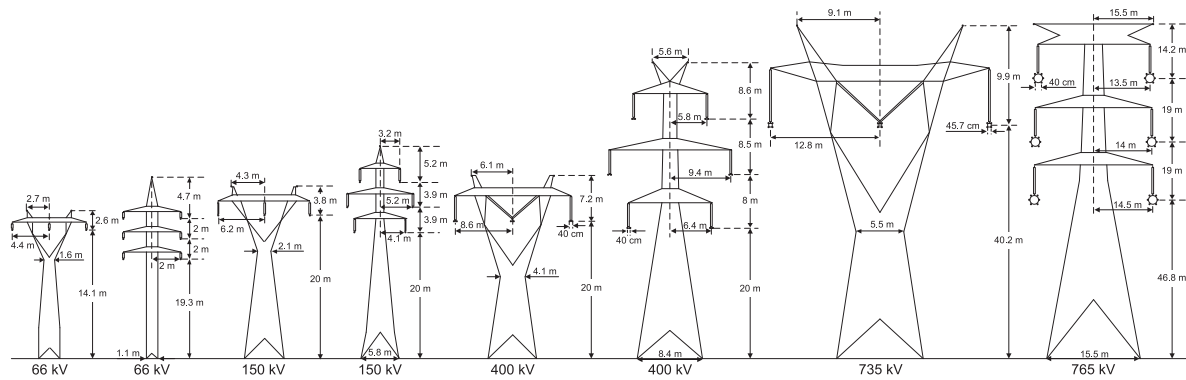
Fig. 1. Tower geometry of the investigated overhead transmission lines (not to scale); adapted from [15].

TABLE I
OVERHEAD TRANSMISSION LINE CHARACTERISTICS

Operating voltage (kV)	No of circuits	Span length (m)	ACSR conductor	Conductor diameter (mm)	Conductors per phase	Conductor sag (m)	OHGW type	OHGW diameter (mm)	OHGW sag (m)	Shielding angle at tower (deg)	Insulator length (m)	BIL (kV)
66	1	250	Raccoon	12.30	1	4.0	Glv steel	6.16	3.0	34.1	0.73	325
66 [45]	2	275	Panther	21.00	1	6.0	Glv steel	9.45	4.0	23.1	0.73	325
150	1	300	Grosbeak	25.15	1	6.3	Glv steel	9.50	4.1	27.3	1.86	750
150	2	300	Grosbeak	25.15	1	6.3	Glv steel	12.60	4.1	31.6	1.86	750
400	1	350	Cardinal	30.42	2	8.6	Glv steel	12.60	5.5	19.2	3.62	1425
400	2	350	Cardinal	30.42	2	8.6	Glv steel	12.60	5.5	19.2	3.62	1425
735 [46]	1	500	Bersfort	35.56	4	25.6	Glv steel	12.57	24.1	20.5	4.80	1950
765 [47]	2	500	Cardinal	30.42	6	18.8	AWS 200	18.50	15.0	−8.0	4.80	1950

OHGW: Overhead Ground Wire, *BIL*: Basic Insulation Level

Adapted from [15]

CIGRE and double-peak waveforms may approximate better recorded lightning currents. However, studies on the effects of applying these two waveforms to OHL simulations have shown that results may vary under the same waveform parameters [8], [14]. Most importantly, the use of recorded waveforms in simulations may yield overvoltages and critical lightning currents causing OHL insulation flashover differing considerably from those obtained by the CIGRE and double-peak waveforms. This may have significant implications in the computed lightning flashover rate of OHLs.

This work investigates the application of recorded lightning current waveforms to the estimation of overvoltages and critical lightning currents causing flashover to OHLs through electromagnetic transient simulations. Typical OHLs are simulated with power frequency voltage from 66 kV up to 765 kV and horizontal (single-circuit), as well as vertical (double-circuit) phase configurations. Backflashover and shielding failure flashover simulations were performed in ATP-EMTP [40], [41] software for several recorded first return-stroke current waveforms of negative downward lightning flashes, as reported in literature [42], [43], [44]. Simulations were also carried out with the widely-used CIGRE lightning current waveform, by approximating the recorded waveforms and considering statistical distributions of front time, maximum steepness, and time to half value; thus, the adequacy of the CIGRE waveform in representing recorded waveforms is examined. Also, a comparison between double-peak waveforms and their CIGRE approximations is performed for the OHLs under study (66 kV up to 765 kV), differing significantly in characteristics, thus, allowing for generalization of results. Finally, the criterion for terminating leader propagation (withstand of insulation) employed in the extensively applied

leader development models for predicting the impulse behavior of insulators and long air gaps is assessed.

II. INVESTIGATED OVERHEAD TRANSMISSION LINES (OHLs)

Fig. 1 depicts the towers of the investigated typical OHLs (66 kV to 765 kV). Both horizontal (single-circuit) and vertical (double-circuit) phase configurations were considered for each voltage level. Table I lists the basic characteristics of these lines. Preliminary results have been presented in [48] for the 150 kV double-circuit OHL.

III. LIGHTNING CURRENT WAVEFORMS UNDER STUDY

Several recorded negative first return-stroke current waveforms have been reported in literature, obtained through direct lightning current measurements at instrumented towers [26]. A large number of recorded waveforms have been gathered and digitized. Six of them were selected considering their parameters [48], so as to be employed in systematic simulations of lightning surges on the OHLs of Fig. 1. The selected recorded current waveforms are depicted in Fig. 2 and their parameters, as defined according to CIGRE [28], [29] (Fig. 12 of Appendix A), are given in Table II.

Fig. 2 also includes approximations of the recorded lightning currents with the waveform proposed by CIGRE WG 33.01 [28]. This waveform is widely adopted in studies dealing with direct lightning strikes, since it can reproduce the upwardly concave wavefront of recorded negative first return-stroke currents. For this purpose, the sum of a linear and a power function is used up to the wavefront point corresponding to 90% of the peak current.
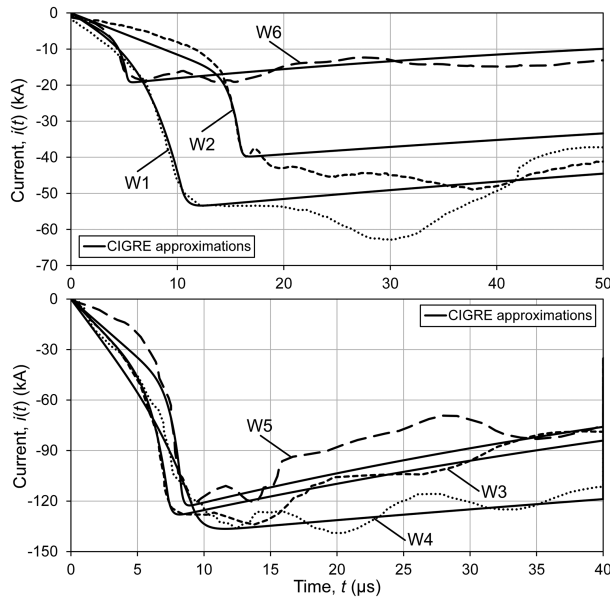
Fig. 2. Recorded first return-stroke current waveforms W1-W6 of negative downward lightning flashes and CIGRE waveform approximations (solid lines). Waveform parameters: Table II.

TABLE II
WAVEFORM PARAMETERS OF THE RECORDED FIRST RETURN-STROKE CURRENTS EMPLOYED IN SIMULATIONS

Waveform	Source		I_I (kA)	I_F (kA)	t_{d30} (µs)	S_m (kA/µs)	t_h (µs)
W1	Berger Fig. 15 of [42]	no. 6235, (1)	53.4	63.0	7.1	18.5	151.0
W2		no. 6236, (2)	39.8	48.9	5.5	25.5	139.4
W3	Narita et al. Fig. 5 of [43]	(1)	128.2	134.2	5.3	55.0	52.5
W4		(2)	136.5	139.0	9.1	21.8	120.6
W5		(3)		122.6	3.7	78.1	46.0
W6	Takami & Okabe Fig. 5(a) of [44]		18.8	19.2	3.4	14.5	62.2

Definitions of waveform parameters according to CIGRE [28], [29] (Section III, Fig. 12, Appendix A). I_I: initial (first) lightning current peak, I_F: final (second) lightning current peak (usually $I_F > I_I$), t_{d30}: front time, S_m: maximum steepness, and t_h: time to half value.

The remaining wavefront up to the peak and the wavetail of the waveshape are described by a double-exponential function. Hence, there is a transition point between the two functions, where the derivative of the current is not continuous; this could be a drawback in some cases. In addition, due to this transition point, caution should be exercised in the selection of the CIGRE waveform input parameters, as an inappropriate selection could cause a discontinuity on the current waveform as well.

The input parameters for the CIGRE waveform are (Fig. 12 of Appendix A): i) the peak current, I_F, ii) the front time, t_{d30}, iii) the maximum steepness, S_m, and iv) the time to half value, t_h. t_{d30} is equal to $(t_{90\%} - t_{30\%})/0.6$, where $t_{90\%}$ and $t_{30\%}$ refer to the points on the wavefront corresponding respectively to 30% and 90% of I_F; S_m is set at the latter point. t_h is the time interval up to the wavetail point corresponding to 50% of I_F. Therefore, each CIGRE waveform is described by the set of parameters: (I_F, t_{d30}, S_m, t_h).

TABLE III
INVESTIGATED CASES OF FIRST RETURN-STROKE CURRENT WAVEFORMS OF NEGATIVE DOWNWARD LIGHTNING FLASHES

Case	Waveform	Parameters	Information
W1-W6	Recorded	Table II	Table II, Fig. 2
W1-W6 approximation	CIGRE	Approximation of the recorded waveforms (Fig. 2)	
Best-case scenario	CIGRE	$(t_{d30,5\%}, S_{m,95\%}, t_{h,95\%})$ Table IV	Highest critical current
Worst-case scenario		$(t_{d30,95\%}, S_{m,5\%}, t_{h,5\%})$ Table IV	Lowest critical current
Median parameters		$(t_{d30,50\%}, S_{m,50\%}, t_{h,50\%})$ Table IV	Commonly used in lightning performance studies
Double-peak MC, MSS	Double-peak	Median parameters MC and MSS Table V	Morro do Cachimbo (MC) & Mount San Salvatore (MSS) instrumented towers
Double-peak approximation with single-peak	CIGRE	Approximation of the double-peak waveforms with single-peak waveforms	

Three more sets of parameter were selected for the CIGRE waveform (Table III), in addition to those approximating the recorded waveforms of Fig. 2 and Table II. These sets consider the log-normal approximations of the statistical distributions of negative first return-stroke parameters, as given in Table IV [28], [49]. Percentages, used at the subscripts of the waveform parameter sets of Table III, denote cases exceeding the parameter value tabulated in Table IV. The first two sets, $(t_{d30,5\%}, S_{m,95\%}, t_{h,95\%})$ and $(t_{d30,95\%}, S_{m,5\%}, t_{h,5\%})$ are associated respectively with long wavefront, low steepness, and short wavetail and vice versa. Therefore, these sets represent the best- and worst-case scenarios, respectively, for overvoltages, thus also for critical currents [49]. The best-case set yields the highest critical current (lowest overvoltage) and the worst-case set the lowest critical current (highest overvoltage). Consequently, the former yields optimistic lightning flashover rate estimates and the latter pessimistic (conservative). In addition, it is noted that the distributions of t_{d30} and S_m are conditional for a given I_F and, thus, t_{d30} and S_m vary with I_F (Table IV). Median values ($t_{d30,50\%}$, $S_{m,50\%}, t_{h,50\%}$) were adopted as the last set of CIGRE waveform parameters, as commonly used for the estimation of the lightning performance of OHLs.

Simulations were also performed for double-peak lightning current waveforms [29], [35] (Table III). The latter are described by a sum of seven Heidler functions [33], [34] enabling the reproduction of the upwardly concave wavefront, as well as of the second higher peak of recorded negative first return-stroke currents. Thus, generating a specific waveform requires determining the values of 28 parameters, 4 for each Heidler function; specialized algorithms may be used for this purpose [29], [50]. This is a drawback as compared with the CIGRE waveform, which can be easily used in parametric investigations, since only lightning current waveform parameters are needed. An advantage of the double-peak waveform is the continuous first derivative of the current due to the single expression used for the whole current duration. In this work, two sets of waveform parameters were selected (Tables III and V) for the comparison of simulation results obtained using double-peak waveforms and their CIGRE approximations. These sets correspond to

TABLE IV
LOG-NORMAL DISTRIBUTIONS OF WAVEFORM PARAMETERS FOR FIRST RETURN-STROKES OF NEGATIVE DOWNWARD LIGHTNING FLASHES [28] AND % OF CASES
EXCEEDING TABULATED VALUES

Waveform parameter	Median value, M	Logarithmic standard deviation, β	95%	50%	5%	Range of peak current, I_F
t_{d30} (µs)	$1.77 \cdot I_F^{0.188}$ $0.906 \cdot I_F^{0.411}$	0.494	$0.785 \cdot I_F^{0.188}$ $0.402 \cdot I_F^{0.411}$	$1.770 \cdot I_F^{0.188}$ $0.906 \cdot I_F^{0.411}$	$3.989 \cdot I_F^{0.188}$ $2.042 \cdot I_F^{0.411}$	$3 \leq I_F \leq 20$ kA $I_F > 20$ kA
S_m (kA/µs)	$12 \cdot I_F^{0.171}$ $6.5 \cdot I_F^{0.376}$	0.554	$4.824 \cdot I_F^{0.171}$ $2.613 \cdot I_F^{0.376}$	$12 \cdot I_F^{0.171}$ $6.5 \cdot I_F^{0.376}$	$29.849 \cdot I_F^{0.171}$ $16.168 \cdot I_F^{0.376}$	$3 \leq I_F \leq 20$ kA $I_F > 20$ kA
t_h (µs)	77.5	0.577	30	77.5	200.2	–

TABLE V
PARAMETERS OF THE DOUBLE-PEAK WAVEFORMS EMPLOYED IN SIMULATIONS

Waveform	Source		I_I (kA)	I_F (kA)	t_{d30} (µs)	S_m (kA/µs)	t_h (µs)
MC	De Conti & Visacro Table III of [35]	Morro do Cachimbo	40.1	45.3	5.00	20.2	53.8
MSS		Mount San Salvatore	27.8	31.0	3.83	24.4	75

Definitions of waveform parameters according to CIGRE [28], [29] (Section III, Fig. 12, Appendix A). I_I: initial (first) lightning current peak, I_F: final (second) lightning current peak (usually $I_F > I_I$), t_{d30}: front time, S_m: maximum steepness, and t_h: time to half value.
The values of the 28 required parameters for generating the double-peak waveforms can be found in Tables I and II of [35].
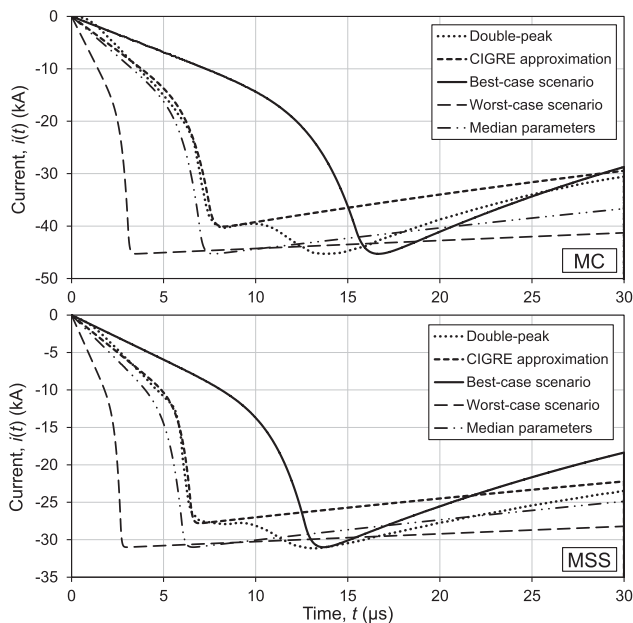

Fig. 3. Double-peak first return-stroke current waveforms of negative downward lightning flashes and CIGRE waveforms (Table III). Waveform parameters: Median values from Morro do Cachimbo (MC) & Mount San Salvatore (MSS) instrumented towers (Table V).

median values of lightning current field data for negative first return-strokes measured at the instrumented towers located at Morro do Cachimbo (MC) and Mount San Salvatore (MSS) [35]. The waveforms under study are shown in Fig. 3.

IV. SIMULATION RESULTS AND DISCUSSION

ATP-EMTP [40], [41] simulations were conducted for the cases of Table III to evaluate the effects of recorded (Fig. 2

and Table II) and double-peak (Fig. 3 and Table V) lightning current waveforms on the estimated overvoltages and critical lightning currents causing flashover to typical OHLs (Fig. 1). The modeling approach of this work, adopted from [12], [15], [51], is described in Table VI of Appendix B. Preliminary results for the 150 kV double-circuit OHL have been presented in [48].

The estimation of the critical (minimum) lightning currents causing backflashover and shielding failure flashover of OHL insulation requires scaling up and down, as necessary, the recorded and double-peak lightning current waveforms and their CIGRE approximations (Figs. 2 and 3, Tables II and V). In an effort to keep waveform scaling to a minimum, a single value of power frequency tower ground resistance, R_g, was adopted for each OHL and waveform (recorded or double-peak) combination. Thus, the critical flashover current value is relatively close to the original lightning current peak, distorting each waveform as little as possible. Also, for the same reasons, W6 waveform (Table II) was the only used for shielding failure investigations due to its lowest peak current; for shielded lines, the maximum lightning current that may terminate on a phase conductor [52] is usually at the lower end of lightning peak currents.

A. Comparison of Recorded and CIGRE Waveforms

1) Backflashover Simulations: Fig. 4 depicts computed overvoltages at the outer phase insulators of the 150 kV single-circuit OHL (Fig. 1) normalized with BIL (750 kV, Table I). These illustrative overvoltages were obtained for the lightning current waveforms of the recorded (W1-W6, Table II) and CIGRE cases under study (Table III) injected at the tower when the AC voltage of the outer phase obtains its positive peak value. Thus, worst-case conditions for backflashover are established. The overvoltages of Fig. 4 result in withstand of insulators as the lightning peak current was lower than the critical value. Note that results for the 150 kV double-circuit OHL (Fig. 1) have been given in Fig. 3 of [48].

From Fig. 4, it can be seen that the typical overvoltages vary notably among lightning current waveforms. This exerts a significant influence on the critical (minimum) backflashover current, as will be shown in what follows. The minimum and maximum peak values of the overvoltages of Fig. 4 generally correspond to the worst- and best-case scenarios of Table III. W1 and W2 waveforms are exceptions, as they yield lower overvoltages than those obtained for the best-case CIGRE waveform. In general, the overvoltages for recorded waveforms are lower than those computed for CIGRE approximations; thus, the latter yield
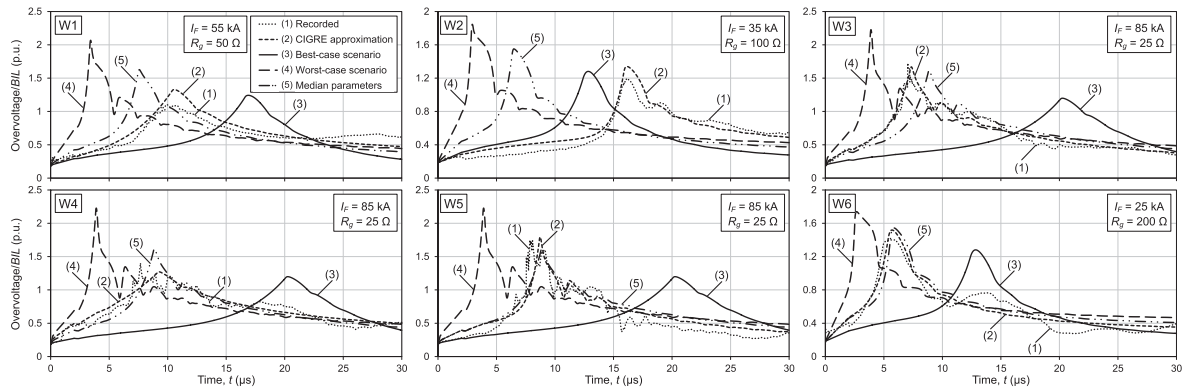
Fig. 4. Normalized overvoltages at the outer insulator of the 150 kV single-circuit line of Fig. 1 for the lightning current waveforms of the recorded (W1-W6, Table II) and CIGRE cases under study (Table III); withstand cases for lightning strikes at the tower at the positive peak value of the outer phase.

conservative results. Also, greater variations with time can be observed on the overvoltage waveforms for recorded lightning currents; this is enhanced close to the peak and on the wavetail.

Fig. 5 depicts the estimated minimum backflashover current, I_{BF}, of the OHLs of Fig. 1 for the recorded (W1-W6, Table II) and CIGRE waveform cases (Table III). The I_{BF} results of Fig. 5 correspond to threshold (lowest) values, associated with worst-case conditions for backflashover, that is, positive peak AC voltage of the outer and lower phase conductors of the single- and double-circuit lines, respectively, at the instant of lightning strike. From Fig. 5 it is evident that CIGRE approximations generally yield conservative I_{BF} values (up to 20% lower) as compared with recorded waveforms. This is slightly more pronounced for the 66 kV lines, most probably due to the lower insulation level and tower ground resistance, R_g, employed in simulations. It is noted that conservative I_{BF} values for CIGRE approximations were also found when using higher or lower R_g values than those of Fig. 5, that is, when scaling the waveforms up and down to a large extent. The results of the W4 waveform for the 66 kV double-circuit line are an exception to the above, mainly due to the extremely low tower ground resistance of 1 Ω employed in simulations. This causes a rapid decrease of the overvoltage stressing insulators during the wavetail of the lightning current. When considering the CIGRE approximation of W4, leader development and, hence, flashover are impeded. This is not the case for W4 waveform owing to abrupt fluctuations at the wavetail of the overvoltage, under which, however, leader development is sustained.

The lower critical current for CIGRE approximations (Fig. 5) is due to higher overvoltages stressing insulators, as seen in Fig. 4 for the 150 kV single-circuit OHL. The recorded lightning current waveforms attain the maximum current value at the second peak (I_F in Fig. 12 of Appendix A), that is, later than their CIGRE approximations (Fig. 2). The single peak of the latter coincides with the first (lower) peak of recorded waveforms (I_I in Fig. 12 of Appendix A), which is typically used to define their wavefront parameters [28], [29] (Fig. 12). Hence, CIGRE waveforms approximating recorded ones cause higher overvoltages when scaled up to the same maximum current with recorded waveforms (equal to I_F) due to the shorter time needed to reach the peak value, I_F, resulting in higher steepness. This

is further supported by the opposite behavior of W5 waveform (lower I_{BF} for W5 than its approximation, Fig. 5), which attains the maximum current at the first peak (Fig. 2). The scaled-up CIGRE approximation exhibits a higher average steepness as well, when the steepness is defined with the first peak I_I of the recorded waveform and the peak of the CIGRE waveform (both waveforms having the same maximum current I_F). This is demonstrated in Fig. 6 for the average steepness $S_{30/90}$ (through 30% and 90% intercepts on the wavefront) of the W3 recorded waveform (black dashed line) and its CIGRE approximation scaled up to the same maximum current I_F (grey solid line).

As seen from Fig. 5, the minimum and maximum I_{BF} values were generally computed for the CIGRE waveforms associated with the worst- and best-case scenarios of Table III, in line with the overvoltage results of Fig. 4. I_{BF} for the best-case scenario is typically up to ~65% higher than the worst case, with even higher differences being observed in some cases. It is noted, however, that higher I_{BF} values may be obtained for recorded than the best-case scenario lightning current waveforms, e.g., for W1 in Fig. 5. Moreover, it is important that median parameters (Table III) yield I_{BF} values between the worst- and best-case scenarios being relatively closer to the worst case.

The differences among the estimated I_{BF}, as obtained using recorded and CIGRE waveforms, would certainly affect the backflashover rate of the OHLs, especially for higher I_{BF} values due to their lower probability of occurrence.

2) Shielding Failure Simulations: The overvoltage waveform across insulators computed for the shielding failure case is essentially the same with the waveform of the lightning current, as surges propagate in both directions of the OHL without reflections. The estimated critical (minimum) shielding failure flashover current, I_c, was not affected appreciably by the examined waveform cases of Table III, with maximum differences ~3% between extreme cases (best- and worst-case scenarios, Table III) for each OHL. I_c values for the recorded W6 waveform, CIGRE approximation, and median parameters are closer to the worst case for most OHLs. The differences among the estimated I_c, as obtained using recorded and CIGRE waveforms, would affect the shielding failure flashover rate of the OHLs, depending on the effectiveness of their shielding design.
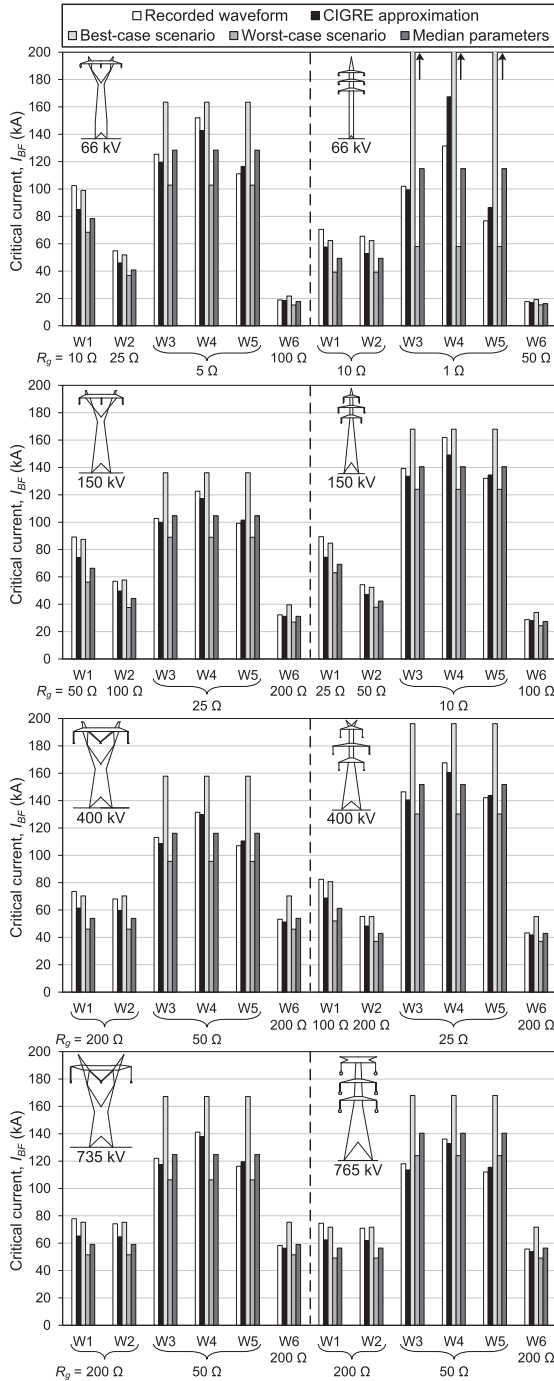
Fig. 5. Minimum backflashover current, I_{BF}, (threshold values) of the overhead lines of Fig. 1 for the recorded (W1-W6, Table II) and CIGRE waveform cases under study (Table III).
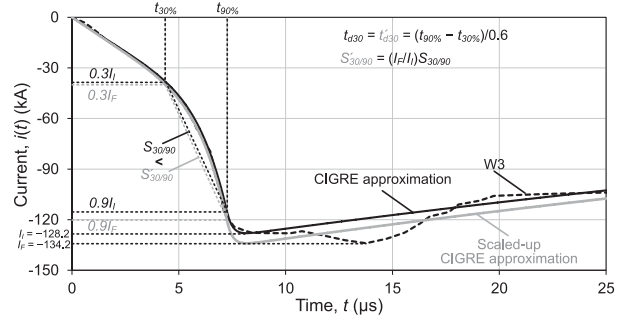

Fig. 6. Recorded lightning current waveform W3 (Table II) (black dashed line) and its CIGRE approximation (black solid line) with a maximum current equal to the first peak of W3, I_I. Grey solid line denotes the CIGRE approximation scaled up to the maximum current of W3 waveform (I_F, second peak).
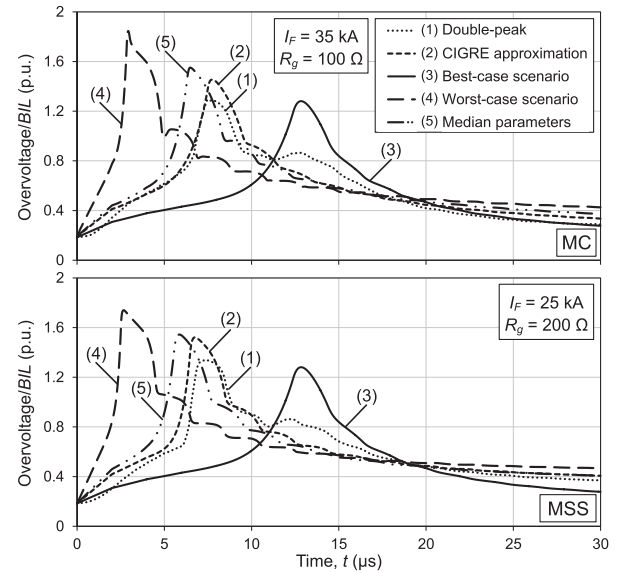

Fig. 7. Normalized overvoltages at the outer insulator of the 150 kV single-circuit line (Fig. 1) for the double-peak and CIGRE waveform cases under study (MC and MSS median values, Tables III and V); withstand cases for lightning strikes to the tower at the positive peak value of the outer phase.

B. Comparison of Double-Peak and CIGRE Waveforms

Fig. 7 presents computed overvoltages at the outer phase insulators of the 150 kV single-circuit OHL of Fig. 1 for the double-peak and CIGRE waveforms (Tables III and V). These typical overvoltages (withstand cases) were obtained for worst-case conditions regarding backflashover. The corresponding overvoltages for the 150 kV double-circuit OHL (Fig. 1) have been depicted in Fig. 2 of [48].

From Fig. 7, it is evident that the typical overvoltages due to double-peak waveforms are much lower than their CIGRE approximations. This results in considerably lower minimum backflashover current, I_{BF}, for the latter case, as shown in Fig. 8 for all cases under study (Table III) and OHLs (Fig. 1). Thus, CIGRE (single-peak) approximations of the double-peak waveforms yield conservative results, as for the recorded waveforms case (Section IV.A.1); this is also the case for higher or lower R_g values. In fact, I_{BF} values lower up to ∼10% (8% on average) were obtained (Fig. 8); differences are generally more pronounced for single-circuit lines and for lines of lower operating voltage.

It is noteworthy that the results of Figs. 7 and 8 for the OHLs of Fig. 1 (66 kV up to 765 kV) are in line with those of [8] and [14] where higher overvoltages and lower I_{BF} values were obtained for the CIGRE waveforms as compared with double-peak waveforms under the same current parameters. Actually, I_{BF} for the CIGRE waveform was reported 7% lower
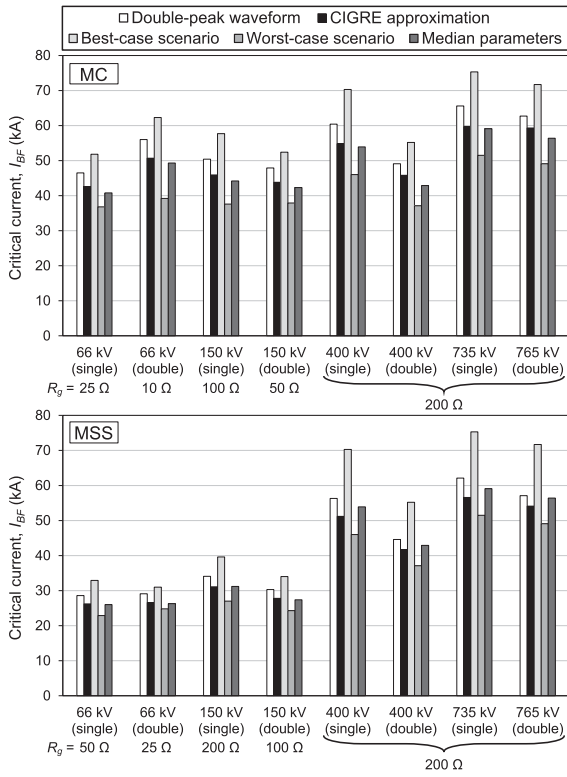
Fig. 8. Minimum backflashover current, I_{BF}, (threshold values) of the overhead lines of Fig. 1 for the double-peak and CIGRE waveform cases under study (MC and MSS median values, Tables III and V).

for a 500 kV OHL with horizontal phase configuration in [8]. Lower I_{BF} values up to 3% were found from [14] for 138 kV and 230 kV single-circuit OHLs with vertical and horizontal phase configurations, respectively.

As evident from Fig. 8, I_{BF} for double-peak waveforms and CIGRE approximations lies in the range defined by the limiting I_{BF} values for the worst- and best-case scenarios of Table III. Also, I_{BF} results for median parameters (CIGRE distributions [28], Table IV) are comparable to the CIGRE approximation for the Mount San Salvatore (MSS) median values case [35], as these are based on the same set of field data. For the Morro do Cachimbo (MC) case, I_{BF} for the CIGRE median parameters is lower than that for the CIGRE approximation, because the MC median values correspond to longer and less steep wavefronts (Fig. 3, Table V) resulting in lower overvoltages (Fig. 7).

V. DISCUSSION ON LEADER DEVELOPMENT MODELS

Several models have been proposed for the evaluation of the dielectric strength of overhead transmission line insulation (long air gaps and insulators) under switching [53], [54], [55], [56] and lightning impulses [1], [2], [3], [5], [28], [29], [30], [31], [32], [55], [56], [57], [58], [59], [60], [61]. This separate classification is due to the considerable differences in breakdown mechanism caused by the different impulse duration, being much shorter for lightning impulses. Hence, in this case modeling is based on the final jump phase, as leader propagates with increasing velocity in the already bridged gap by partially conducting streamers [55].
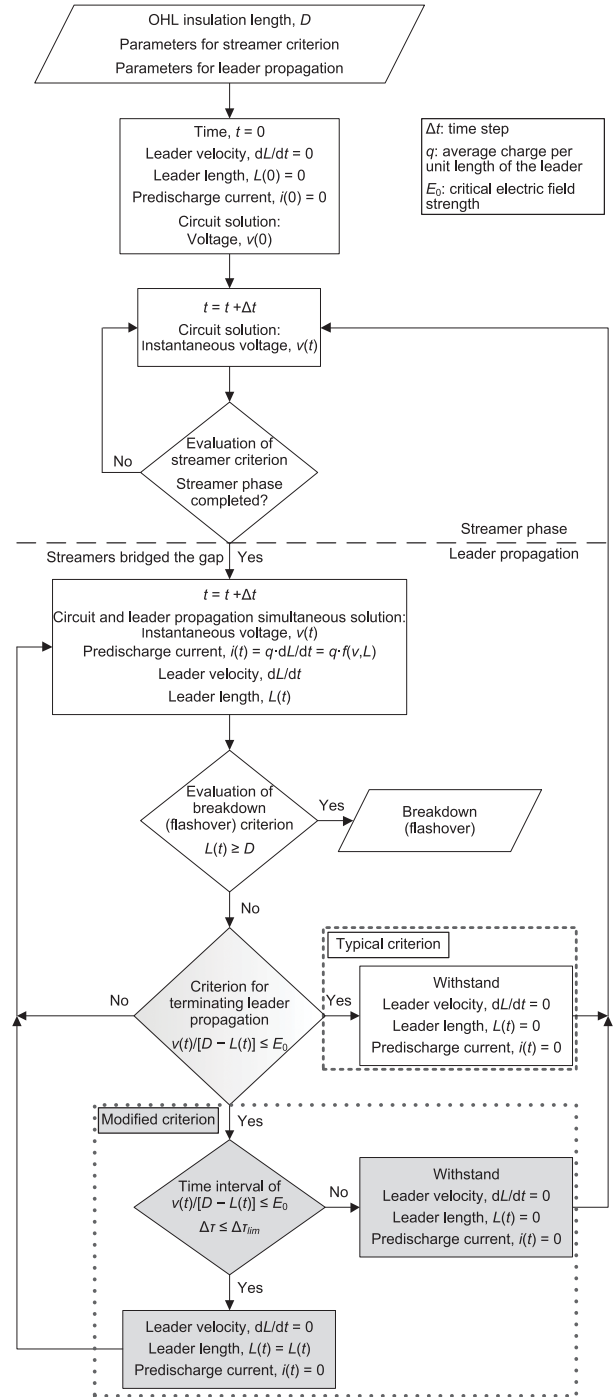

Fig. 9. Flowchart for the application of leader development models for predicting the impulse behavior of OHL insulation. Both the typical and the modified leader development termination criteria are shown.

With respect to lightning impulses, leader development models [5], [28], [29], [30], [31], [55], [56], [57], [58], [59], [60], [61] are used in electromagnetic transient simulations for predicting the impulse behavior of OHL insulation, that is, breakdown of long air gaps and insulator flashover. These models consider the physical mechanism of electrical breakdown to evaluate the effects of non-standard overvoltage waveforms stressing OHL insulation. Actually, as shown in Fig. 9, two phases are

considered: streamer phase and leader propagation. The former is usually assumed to be completed when the average gradient in the gap reaches a critical value, E_0 [28], [57]; other criteria are discussed in [60]. Then, leader propagation begins based on its velocity, dL/dt (Fig. 9). This phase is completed by breakdown or withstand of insulation. The former occurs when leader crosses the gap. Withstand is commonly assumed when the average gradient in the unbridged part of the gap becomes less than the critical, E_0 (typical criterion, dashed box in Fig. 9). Then, leader is considered to be quenched, that is, its length is set to zero ($L = 0$).

A. Analysis on the Leader Development Termination Criterion

Lightning overvoltage waveforms may exhibit abrupt instantaneous fluctuations due to reflections and lightning current variations, as in Figs. 4 and 7 for recorded, double-peak, and CIGRE waveforms (more marked for the former). These perturbations may result in electric field strength values (in the unbridged part of the gap by the leader) lower than the critical for a very short time, $\Delta\tau$. Hence, in this case the leader length is set to zero in simulations. In the actual case, however, the leader may not be quenched and propagate again with the increase of the overvoltage; note that discontinuous leader development has been observed experimentally [28], [57], as shown for example in Fig. C7 of [57] and Fig. 12 of [61]. This can be easily considered in leader development models by modifying the criterion for the termination of leader propagation yielding insulation withstand. Actually, as shown in in the dotted box of Fig. 9, the leader resumes propagating from its last position in the gap if the voltage gradient in the remaining unbridged part becomes again higher than the critical field after a short time interval, $\Delta\tau$.

The determination of the upper limit of this time interval $\Delta\tau_{lim}$ has been performed by considering: i) experimental data from literature on the electrical breakdown of long air gaps and insulators stressed by lightning impulses which present perturbations, such as oscillations or abrupt fluctuations and ii) typical computed or measured non-standard waveforms of lightning overvoltages stressing OHL insulation.

As regards (i), from the results presented in [57] and [61], it can be observed that the leader may halt propagating for a time interval up to ~1 μs. However, $\Delta\tau_{lim}$ is expected to depend on overvoltage characteristics, polarity, and insulation configuration; it could also be subject to statistical variations. In addition, in the same studies, the time duration of the abrupt fluctuations at the wavetail of the applied impulses, $\Delta\tau_f$, (Fig. 10) was in the range of 0.7-2.3 μs [57] and ~3.8 μs [61]. Within this range are also the corresponding $\Delta\tau_f$ values obtained from the computed overvoltages on the overhead lines of Fig. 1 and Table I [point (ii)]. Generally, $\Delta\tau_f$ values lower than ~2 μs have been computed for the evaluated systems of Fig. 1, decreasing with increasing tower ground resistance, with an upper limit of ~3.5 μs. Comparable $\Delta\tau_f$ values were also found from measured [62] and computed [4], [8], [12], [13], [14], [15], [17], [20], [22], [49], [51], [58], [59], [63], [64], [65], [66], [67], [68], [69] overvoltage waveforms reported in literature. Since $\Delta\tau_{lim}$ is reasonably shorter than $\Delta\tau_f$, a value of 2 μs was deemed
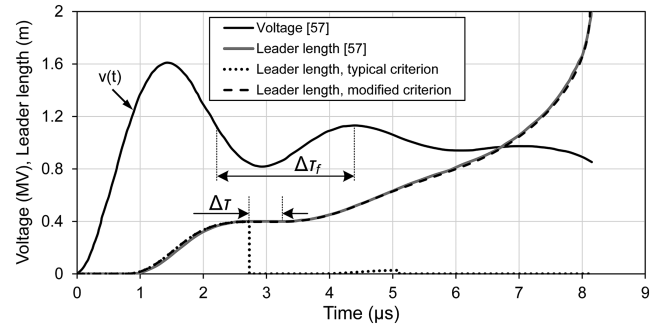

Fig. 10. Simulation results on the prediction of the impulse behavior of a 2 m rod-plane gap; solid lines: Fig. C7 of [57].
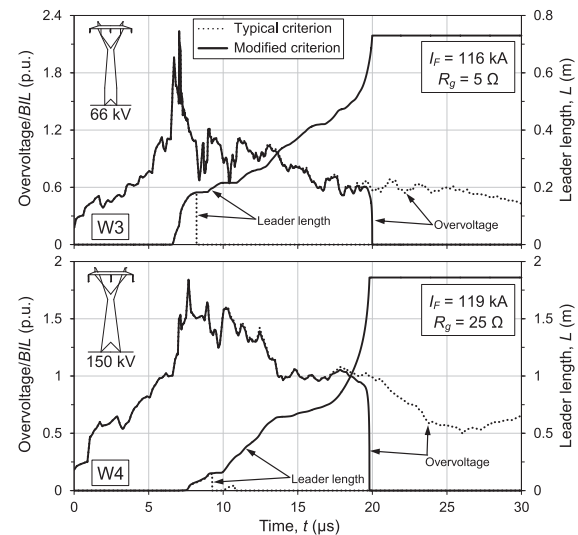

Fig. 11. Normalized computed overvoltages at the outer insulators of the 66 kV and 150 kV single-circuit overhead lines of Fig. 1 and leader length for the typical and modified leader termination criteria of Fig. 9; worst-case conditions for backflashover when using the modified criterion; lightning currents: waveforms W3 and W4 (Table II) for the 66 kV and 150 kV lines, respectively.

appropriate for the former. Certainly, more experimental work is required to shed light to this parameter and its influencing factors.

B. Simulation Results and Discussion

Fig. 10 shows simulation results for the case of Fig. C7 of [57] using both the common and modified criteria. The original results are reproduced for the modified criterion. The latter was applied to backflashover simulations for recorded and double-peak waveforms and CIGRE approximations (Tables II, III, and V) as abrupt changes were not observed in the computed shielding failure overvoltages. Fig. 11 depicts typical computed overvoltages at the outer insulators of the 66 kV and 150 kV single-circuit OHLs (Fig. 1) normalized with BIL (325 kV and 750 kV, respectively, Table I) for lightning strikes to the tower. Both the typical and modified leader termination criteria of Fig. 9 were used. The lightning current was equal to the critical backflashover current, I_{BF}, corresponding to the modified criterion case. W3 and W4 recorded lightning current waveforms

(Table II) were applied to the 66 kV and 150 kV OHLs, respectively. The computed values of the leader length are included as well. The effect of the modified criterion on leader propagation is evident (discontinuous leader development), resulting in a lower I_{BF}. Actually, the latter is equal to 116 kA and 119 kA for the 66 kV and 150 kV OHLs, respectively, as shown in Fig. 11. The corresponding values for the typical criterion are 125 kA and 123 kA.

Lower critical backflashover currents may be obtained for the modified more realistic criterion, depending on the extent of overvoltage variations and the rate of decrease during the wavetail. In fact, lower I_{BF} values up to ~15%, 10%, and 5% were observed respectively for the recorded, double-peak and CIGRE approximation waveforms. CIGRE approximations still yield conservative results for the modified criterion. Also, the effects of the modified criterion are less marked for single-circuit OHLs. The differences in I_{BF} decrease notably with increasing OHL operating voltage and ground resistance due to smoother overvoltage waveforms.

In light of the above, the modified criterion shall apply to cases with abrupt overvoltage variations and a high rate of decrease during the wavetail. These include OHLs of lower operating voltage and for relatively low tower ground resistance (lower than 25 Ω for the evaluated lines), as the estimation of their lightning performance may be affected by the use of the modified criterion. Nevertheless, since the implementation of this criterion in leader development models code is straightforward and does not impose computational burden, it is suggested to be used in all cases.

VI. CONCLUSION

The effects of recorded lightning current waveforms on the overvoltages and critical lightning currents causing flashover to overhead transmission lines have been studied via ATP-EMTP simulations. Backflashover and shielding failure simulations were performed for typical 66-765 kV single- and double-circuit lines. Several recorded negative first return-stroke current waveforms from literature were evaluated. CIGRE lightning current waveforms approximating recorded and double-peak waveforms were used in simulations, considering also statistical distributions of waveform parameters.

Approximating recorded and double-peak waveforms with CIGRE waveforms generally yields conservative overvoltages and critical backflashover current (lower values); the latter is up to ~20% and 10% lower for the CIGRE approximation of recorded and double-peak waveforms, respectively. These effects are slightly more pronounced for lower voltage lines. They are attributed to the single peak I_F of CIGRE approximations, which causes higher overvoltages due to higher wavefront steepness as the single peak I_F coincides with the typically lower first peak I_I of recorded and double-peak waveforms ($I_I < I_F$). Thus, the duration to peak I_F of CIGRE approximations is shorter than that to the typically higher second peak I_F of recorded and double-peak waveforms. It is important to note that quantitative results on overvoltages and critical currents depend on the examined recorded lightning current waveforms.

Qualitative results, however, are expected to hold in general except for a few cases, such as the W5 recorded waveform of this work exhibiting the maximum current at the first peak and not at the second as usual. In such cases, a higher critical current may be obtained for the CIGRE approximation.

The minimum and maximum critical backflashover currents have been obtained for the CIGRE waveforms associated with the worst- and best-case scenarios regarding insulation flashover, that is, a current waveshape of short wavefront, high steepness, and long wavetail for the former scenario and vice versa for the latter. These scenarios were selected based on the distributions of waveform parameters. The critical current is up to ~65% higher for the best case; values even higher may be obtained for recorded waveforms. CIGRE waveforms with median parameters yield results closer to the worst case. The effects on the critical shielding failure flashover current are minimal with maximum differences ~3% between extreme cases.

The overvoltages computed for lightning strikes to towers may exhibit abrupt fluctuations of short duration due to reflections and lightning current variations, being enhanced for recorded waveforms. Hence, the common criterion employed in leader development models for the termination of leader propagation (withstand of line insulation) may yield relatively high critical backflashover current. This is because the leader is considered to be quenched at the instant the voltage gradient in the unbridged part of the gap becomes lower than a critical value. A more realistic criterion has been evaluated according to which the leader length does not become zero instantaneously and leader resumes propagating from the last length if the gradient becomes higher than the critical again after a short time interval. A recommendation of an upper limit of 2 μs for this interval is made based on literature results. When using this modified criterion, critical currents lower up to 15% have been obtained. Thus, this modified criterion shall apply to cases with abrupt overvoltage variations and a high rate of decrease during the wavetail, such as for overhead lines with lower operating voltage, low tower ground resistance values, and fast lightning current waveforms. Nevertheless, since the implementation of this criterion is straightforward and does not increase computational complexity, it is suggested to be used in all cases.
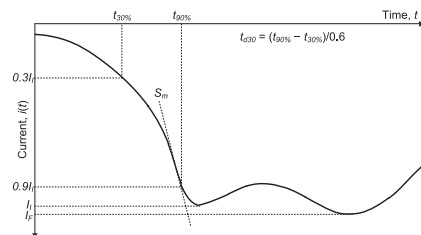
APPENDIX A

Fig. 12. Schematic diagram showing the definitions of negative lightning current wavefront parameters according to CIGRE [26], [28], [29].

APPENDIX B

The modeling approach of Table VI is appropriate for the computation of lightning overvoltages and critical flashover

TABLE VI
ATP-EMTP [40], [41] MODELING APPROACH

Component/ Parameter	Description
Overhead line	A JMarti frequency-dependent model [70] for each line span
	Backflashover simulations: 10 spans (66 kV lines: 12 spans)
	Shielding failure simulations: 11 spans (12 JMarti models: the span where lightning terminates is divided in two half-spans)
	Long line sections as terminations (2 JMarti models)
	Soil resistivity: on the basis of grounding system geometry and power frequency tower ground resistance, R_g, used in simulations
AC voltage	Power frequency AC sources at both line ends
Towers	Lossless frequency-independent distributed lines
	Surge velocity: 85% of the speed of light [71]
	Surge impedance: according to [72] (cylindrical and conical approximations for the single- and double-circuit towers of Fig. 1, respectively)
Insulator flashover	CIGRE [28] leader development model with predischarge current [59], [60]; parameters: negative flashover
Tower grounding systems	Power frequency tower ground resistance, R_g, [71] on the basis of the analysis of Subsection II.C of [15] on the effects of tower grounding system modeling on lightning overvoltages and critical backflashover current estimation, considering uncertainties in tower grounding system modeling
	R_g: several values between 1 and 200 Ω
Lightning return-stroke	Norton equivalent
	Recorded [42]-[44], CIGRE [28], [29], and double-peak [29], [35] lightning current waveforms for the cases of Table III.
	Lightning channel impedance [12]:
	(a) 400 Ω for backflashover simulations
	(b) 1000 Ω for shielding failure simulations
	Lightning strike location:
	(a) Backflashover simulations: tower top
	(b) Shielding failure simulations: outer and upper phase conductor at midspan for single- and double-circuit lines of Fig. 1, respectively
	Recorded waveforms:
	• variable digitization time interval reproducing main features of the waveforms
	• linear interpolation
	• implemented via MODELS language [73], [74] using the external pointlist function
Simulation time step	1 ns
Total simulation time	30-50 μs; depending on the case

Adapted from [12], [15], [51].

currents of OHLs. This is substantiated by the good agreement found between i) the critical backflashover average gradient values estimated through EMTP simulations ∼680–760 kV/m [15] and the 700 kV/m value suggested in IEC 60071-2 [75] and ii) the field measurements reported in [62] for a 275 kV double-circuit overhead line and simulated overvoltages; the developed model (Table VI) predicted correctly the observed multiphase backflashover and flashover time. The above further support the validity of the estimated critical flashover currents. Thus, this work forms the basis for the assessment of the lightning performance of overhead transmission lines based on recorded lightning current waveforms.

REFERENCES

[1] A. R. Hileman, *Insulation Coordination for Power Systems*. Boca Raton, FL, USA: CRC Press, 1999.

[2] W. A. Chisholm and J. G. Anderson, "Lightning and grounding," in *EPRI AC Transmission Line Reference Book–200 kV and Above*, 3rd ed. Palo Alto, CA, USA: EPRI, Ch. 6, 2005, pp. 1–94.

[3] J. A. Martinez-Velasco, Ed. *Power System Transients: Parameter Determination*. Boca Raton, FL, USA: CRC Press, 2010.

[4] F. H. Silveira, A. De Conti, and S. Visacro, "Lightning overvoltage due to first strokes considering a realistic current representation," *IEEE Trans. Electromagn. Compat.*, vol. 52, no. 4, pp. 929–935, Nov. 2010.

[5] Z. G. Datsios, P. N. Mikropoulos, and T. E. Tsovilis, "Estimation of the minimum shielding failure flashover current for first and subsequent lightning strokes to overhead transmission lines," *Electric Power Syst. Res.*, vol. 113, pp. 141–150, Aug. 2014.

[6] J. He, X. Wang, Z. Yu, and R. Zeng, "Statistical analysis on lightning performance of transmission lines in several regions of China," *IEEE Trans. Power Del.*, vol. 30, no. 3, pp. 1543–1551, Jun. 2015.

[7] F. M. Gatta, A. Geri, S. Lauria, M. Maccioni, and F. Palone, "Tower grounding improvement versus line surge arresters: Comparison of remedial measures for high-BFOR subtransmission lines," *IEEE Trans. Ind. Appl.*, vol. 51, no. 6, pp. 4952–4960, Nov./Dec. 2015.

[8] A. R. Rodrigues, G. C. Guimarães, M. L. R. Chaves, W. C. Boaventura, D. A. Caixeta, and M. A. Tamashiro, "Lightning performance of transmission lines based upon real return-stroke current waveforms and statistical variation of characteristic parameters," *Electric Power Syst. Res.*, vol. 153, pp. 46–59, Dec. 2017.

[9] E. Volpov and R. Linder, "Application of local environmental data to the lightning performance assessment of the IECo transmission-line network," *IEEE Trans. Power Del.*, vol. 32, no. 6, pp. 2546–2554, Dec. 2017.

[10] Q. Wang, T. Jahangiri, C. L. Bak, F. F. da Silva, and H. Skouboe, "Investigation on shielding failure of a novel 400-kV double-circuit composite tower," *IEEE Trans. Power Del.*, vol. 33, no. 2, pp. 752–760, Apr. 2018.

[11] P. Malicki, S. Papenheim, and M. Kizilcay, "Shielding failure analysis of a hybrid transmission line with AC and DC systems on the same tower," *Electric Power Syst. Res.*, vol. 159, pp. 2–8, Jun. 2018.

[12] Z. G. Datsios, P. N. Mikropoulos, and T. E. Tsovilis, "Effects of lightning channel equivalent impedance on lightning performance of overhead transmission lines," *IEEE Trans. Electromagn. Compat.*, vol. 61, no. 3, pp. 623–630, Jun. 2019.

[13] J. Gholinezhad and R. Shariatinasab, "Time-domain modeling of tower footing grounding systems based on impedance matrix," *IEEE Trans. Power Del.*, vol. 34, no. 3, pp. 910–918, Jun. 2019.

[14] F. H. Silveira and S. Visacro, "Lightning performance of transmission lines: Impact of current waveform and front time on backflashover occurrence," *IEEE Trans. Power Del.*, vol. 34, no. 6, pp. 2145–2151, Dec. 2019.

[15] Z. G. Datsios, P. N. Mikropoulos, and T. E. Tsovilis, "Closed-form expressions for the estimation of the minimum backflashover current of overhead transmission lines," *IEEE Trans. Power Del.*, vol. 36, no. 2, pp. 522–532, Apr. 2021.

[16] B. Salarieh, H. M. J. De Silva, A. M. Gole, A. Ametani, and B. Kordi, "An electromagnetic model for the calculation of tower surge impedance based on thin wire approximation," *IEEE Trans. Power Del.*, vol. 36, no. 2, pp. 1173–1182, Apr. 2021.

[17] F. H. Silveira, F. S. Almeida, and S. Visacro, and G. M. P. Zago, "Influence of the current front time representation on the assessment of backflashover occurrence of transmission lines by deterministic and probabilistic calculation approaches," *Electric Power Syst. Res.*, vol. 197, Aug. 2021, Art. no. 107299.

[18] D. Conceição, I. J. S. Lopes, and R. Alipio, "An investigation into the effect of the probabilistic distribution of lightning current amplitude on a transmission line backflashover rate," in *Proc. 35th Int. Conf. Lightning Protection, XVI Int. Symp. Lightning Protection*, 2021, pp. 1–6.

[19] A. Yamanaka, N. Nagaoka, and Y. Baba, "Lightning surge analysis of HV transmission line: Bias AC-voltage effect on multiphase back-flashover," *IEEE Trans. Power Del.*, vol. 36, no. 6, pp. 3570–3578, Dec. 2021.

[20] A. Yamanaka, N. Nagaoka, and Y. Baba, "EMT analysis of externally gapped line arresters for reducing lightning faults in 77 kV transmission lines," in *Proc. Int. Council Large Elect. Syst. Kyoto Symp.*, 2022, Art. no. C000019.

[21] E. Stracqualursi, R. Araneo, J. B. Faria, P. Burghignoli, A. Andreotti, and B. Kordi, "On the transient analysis of towers: A revised theory based on Sommerfeld-Goubau wave," *IEEE Trans. Power Del.*, vol. 38, no. 1, pp. 309–318, Feb. 2023.

[22] K. Yin et al., "The design and optimization of the down-lead system for a novel 400 kV composite pylon," *IEEE Trans. Power Del.*, vol. 38, no. 1, pp. 420–431, Feb. 2023.

[23] W. Diesendorf, *Insulation Co-Ordination in High-Voltage Electric Power Systems*. London, U.K.: Butterworth, 1974.

[24] V. A. Rakov and M. A. Uman, *Lightning: Physics and Effects*. Cambridge, U.K.: Cambridge Univ. Press, 2003.

[25] Y. Baba and V. A. Rakov, "On the use of lumped sources in lightning return stroke models," *J. Geophys. Res.*, vol. 110, Feb. 2005, Art. no. D03101.

[26] CIGRE Working Group C4.407, "Lightning parameters for engineering applications," CIGRE, Paris, France, Tech. Brochure 549, Aug. 2013.

[27] J. G. Anderson, "Lightning performance of transmission lines," in *Transmission Line Reference Book, 345 kV and Above*, J. J. LaForest, Ed., 2nd ed. Palo Alto, CA, USA: EPRI, 1982, pp. 545–597.

[28] CIGRE Working Group 33.01, "Guide to procedures for estimating the lightning performance of transmission lines," CIGRE, Paris, France, Tech. Brochure 63, Oct. 1991.

[29] CIGRE Working Group C4.23, "Procedures for estimating the lightning performance of transmission lines–New aspects," CIGRE, Paris, France, Tech. Brochure 839, Jun. 2021.

[30] IEEE Task Force, "Modeling guidelines for fast front transients," *IEEE Trans. Power Del.*, vol. 11, no. 1, pp. 493–506, Jan. 1996.

[31] *Insulation Co-ordination – Part 4: Computational Guide to Insulation Co-ordination and Modelling of Electrical Networks*, IEC TR 60071-4, IEC, Geneva, Switzerland, 2004.

[32] A. Ametani and T. Kawamura, "A method of a lightning surge analysis recommended in Japan using EMTP," *IEEE Trans. Power Del.*, vol. 20, no. 2, pp. 867–875, Apr. 2005.

[33] F. Heidler, J. M. Cvetić, and B. V. Stanić, "Calculation of lightning current parameters," *IEEE Trans. Power Del.*, vol. 14, no. 2, pp. 399–404, Apr. 1999.

[34] F. Heidler and J. Cvetić, "A class of analytical functions to study the lightning effects associated with the current front," *Eur. Trans. Elect. Power*, vol. 12, no. 2, pp. 141–150, Mar./Apr. 2002.

[35] A. De Conti and S. Visacro, "Analytical representation of single- and double-peaked lightning current waveforms," *IEEE Trans. Electromagn. Compat.*, vol. 49, no. 2, pp. 448–451, May 2007.

[36] P. Chowdhuri et al., "Parameters of lightning strokes: A review," *IEEE Trans. Power Del.*, vol. 20, no. 1, pp. 346–358, Jan. 2005.

[37] W. R. Gamerota, J. O. Elismé, M. A. Uman, and V. A. Rakov, "Current waveforms for lightning simulation," *IEEE Trans. Electromagn. Compat.*, vol. 54, no. 4, pp. 880–888, Aug. 2012.

[38] F. Koehler and J. Swingler, "Simplified analytical representation of lightning strike waveshapes," *IEEE Trans. Electromagn. Compat.*, vol. 58, no. 1, pp. 153–160, Feb. 2016.

[39] M. Y. Tomasevich, A. C. S. Lima, and R. F. S. Dias, "Approximation of lightning current waveforms using complex exponential functions," *IEEE Trans. Electromagn. Compat.*, vol. 58, no. 5, pp. 1686–1689, Oct. 2016.

[40] *ATP Rule Book*. Portland, OR, USA: Can.-Amer. EMTP Users Group, 1997.

[41] H. W. Dommel, *Electro-Magnetic Transients Program (EMTP) Theory Book*. Portland, OR, USA: Bonneville Power Administ., 1986.

[42] K. Berger, "Novel observations on lightning discharges: Results of research on Mount San Salvatore," *J. Franklin Inst.*, vol. 283, no. 6, pp. 478–525, Jun. 1967.

[43] T. Narita, T. Yamada, A. Mochizuki, E. Zaima, and M. Ishii, "Observation of current waveshapes of lightning strokes on transmission towers," *IEEE Trans. Power Del.*, vol. 15, no. 1, pp. 429–435, Jan. 2000.

[44] J. Takami and S. Okabe, "Observational results of lightning current on transmission towers," *IEEE Trans. Power Del.*, vol. 2, pp. 547–556, Jan. 2007.

[45] M. B. Najjar, O. Jadayel, A. Baarini, and A. Iaaly, "Power magnetic fields exposure evaluation at North Lebanon: GIS application," in *Proc. Environ. Syst. Res. Inst. Int. User Conf.*, 2009, Art. no. 1109.

[46] F. J. Ellert, S. A. Miske Jr., and C. J. Truax, "EHV-UHV transmission systems," in *Transmission Line Reference Book, 345 kV and Above*, J. J. LaForest, Ed., 2nd ed. Palo Alto, CA, USA: EPRI, 1982, pp. 11–62.

[47] J. B. Kim, E. B. Shim, and J. W. Shim, "Switching overvoltage analysis and air clearance design on the KEPCO 765 kV double circuit transmission system," *IEEE Trans. Power Del.*, vol. 15, no. 1, pp. 381–386, Jan. 2000.

[48] D. G. Patsalis, Z. G. Datsios, P. N. Mikropoulos, and T. E. Tsovilis, "Estimation of lightning overvoltages and critical currents causing flashover to a 150 kV overhead transmission line: Effects of recorded lightning current waveforms," in *Proc. IEEE Int. Conf. High Voltage Eng. Appl.*, 2022, pp. 1–4.

[49] Z. G. Datsios, D. G. Patsalis, P. N. Mikropoulos, and T. E. Tsovilis, "Effects of lightning current waveform on the fast-front overvoltages and critical currents causing insulation flashover to a 150 kV overhead transmission line," in *Proc. 36th Int. Conf. Lightning Protection*, 2022, pp. 521–526.

[50] A. J. Oliveira, M. A. O. Schroeder, R. A. R. Moura, M. T. C. de Barros, and A. C. S. Lima, "Adjustment of current waveform parameters for first lightning strokes: Representation by Heidler functions," in *Proc. Int. Symp. Lightning Protection*, 2017, pp. 121–126.

[51] Z. G. Datsios, P. N. Mikropoulos, T. E. Tsovilis, and S. I. Angelakidou, "Estimation of the minimum backflashover current of overhead lines of the Hellenic transmission system through ATP-EMTP simulations," in *Proc. Int. Colloq. Lightn. Power Syst.*, 2016, Art. no. 32.

[52] P. N. Mikropoulos and T. E. Tsovilis, "Lightning attachment models and maximum shielding failure current of overhead transmission lines: Implications in insulation coordination of substations," *IET Gener. Transmiss. Distrib.*, vol. 4, no. 12, pp. 1299–1313, Dec. 2010.

[53] B. Hutzler and D. Hutzler-Barre, "Leader propagation model for predetermination of switching surge flashover voltage of large air gaps," *IEEE Trans. Power App. Syst.*, vol. PAS-97, no. 4, pp. 1087–1096, Jul. 1978.

[54] F. A. M. Rizk, "A model for switching impulse leader inception and breakdown of long air-gaps," *IEEE Trans. Power Del.*, vol. 4, no. 1, pp. 596–606, Jan. 1989.

[55] CIGRE Working Group 33.07, "Guidelines for the evaluation of the dielectric strength of external insulation," CIGRE, Paris, France, Tech. Brochure 72, 1992.

[56] F. A. M. Rizk and G. N. Trinh, *High Voltage Engineering*. Boca Raton, FL, USA: CRC Press, 2014.

[57] A. Pigini, G. Rizzi, E. Garbagnati, A. Porrino, G. Baldo, and G. Pesavento, "Performance of large air gaps under lightning overvoltages: Experimental study and analysis of accuracy of predetermination methods," *IEEE Trans. Power Del.*, vol. 4, no. 2, pp. 1379–1392, Apr. 1989.

[58] X. Wang, Z. Yu, and J. He, "Breakdown process experiments of 110- to 500-kV insulator strings under short tail lightning impulse," *IEEE Trans. Power Del.*, vol. 29, no. 5, pp. 2394–2401, Oct. 2014.

[59] Z. G. Datsios and P. N. Mikropoulos, "Implementation of leader development models in ATP-EMTP using a type-94 circuit component," in *Proc. 32nd Int. Conf. Lightning Protection*, 2014, pp. 735–741.

[60] Z. G. Datsios and P. N. Mikropoulos, "Modeling of lightning impulse behavior of long air gaps and insulators including predischarge current: Implications on insulation coordination of overhead transmission lines and substations," *Electric Power Syst. Res.*, vol. 139, pp. 37–46, Oct. 2016.

[61] A. A. Akopian, V. P. Larionov, and A. S. Torosian, "Sur les tensions de décharge par choc à travers un isolement à haute tension en fonction de la forme de l'onde de tension," CIGRE paper no. 411, 1954.

[62] H. Motoyama, K. Shinjo, Y. Matsumoto, and N. Itamoto, "Observation and analysis of multiphase back flashover on the Okushishiku test transmission line caused by winter lightning," *IEEE Trans. Power Del.*, vol. 13, no. 4, pp. 1391–1398, Oct. 1998.

[63] F. M. Gatta, A. Geri, and S. Lauria, "Backflashover simulation of HV transmission lines with concentrated tower grounding," *Electric Power Syst. Res.*, vol. 73, no. 3, pp. 373–381, Mar. 2005.

[64] F. M. Gatta, A. Geri, S. Lauria, and M. Maccioni, "Backflashover simulation of HV transmission lines with enhanced counterpoise groundings," *Electric Power Syst. Res.*, vol. 79, no. 7, pp. 1076–1084, Jul. 2009.

[65] W. A. Chisholm, J. G. Anderson, A. Phillips, and J. Chan, "Lightning performance of compact lines," in *Proc. 10th Int. Symp. Lightning Protection*, 2009, pp. 45–64.

[66] W. A. Chisholm, "New challenges in lightning impulse flashover modeling of air gaps and insulators," *IEEE Elect. Insul. Mag.*, vol. 26, no. 2, pp. 14–25, Mar./Apr. 2010.

[67] F. H. Silveira, S. Visacro, and A. De Conti, "Lightning performance of 138-kV transmission lines: The relevance of subsequent strokes," *IEEE Trans. Electromagn. Compat.*, vol. 55, no. 6, pp. 1195–1200, Dec. 2013.

[68] A. Mackow, M. Nilges, M. Kizilcay, and D. Potkrajac, "Analysis of backflashover across insulator strings of a multi-circuit transmission tower with AC and DC systems," in *Proc. Eur. Electromagn. Transients Prog.-Altern. Transients Prog. Conf.*, 2014, pp. 1–12.

[69] S. Visacro and F. H. Silveira, "Lightning performance of transmission lines: Methodology to design grounding electrodes to ensure an expected outage rate," *IEEE Trans. Power Del.*, vol. 30, no. 1, pp. 237–245, Feb. 2015.

[70] J. R. Marti, "Accurate modelling of frequency-dependent transmission lines in electromagnetic transient simulations," *IEEE Trans. Power App. Syst.*, vol. PAS-101, no. 1, pp. 147–157, Jan. 1982.

[71] IEEE WG on Lightning Performance of TL, "A simplified method for estimating lightning performance of transmission lines," *IEEE Trans. Power App. Syst.*, vol. PAS-104, no. 4, pp. 919–932, Jul. 1985.

[72] M. A. Sargent and M. Darveniza, "Tower surge impedance," *IEEE Trans. Power App. Syst.*, vol. PAS-88, no. 5, pp. 680–687, May 1969.

[73] L. Dubé, "MODELS in ATP, Language manual," 1996.

[74] L. Dubé, "Users' Guide to MODELS in ATP," 1996.

[75] *Insulation Co-ordination–Part 2: Application Guidelines*, IEC 60071-2, IEC, Geneva, Switzerland, 2018.